Lab on a Chip

CRITICAL REVIEW

View Article Online
View Journal | View Issue

Cite this: *Lab Chip*, 2016, **16**, 1797

Chemistry pumps: a review of chemically powered micropumps

Chao Zhou,[a] Hua Zhang,[b] Zeheng Li[a] and Wei Wang*[a]

Lab-on-a-chip devices have over recent years attracted a significant amount of attention in both the academic circle and industry, due to their promise in delivering versatile functionalities with high throughput and low sample amount. Typically, mechanical or electrokinetic micropumps are used in the majority of lab-on-a-chip devices that require powered fluid flow, but the technical challenges and the requirement of external power associated with these pumping devices hinder further development and miniaturization of lab-on-a-chip devices. Self-powered micropumps, especially those powered by chemical reactions, have been recently designed and can potentially address some of these issues. In this review article, we provide a detailed introduction to four types of chemically powered micropumps, with particular focus on their respective structures, operating mechanisms and practical usefulness as well as limitations. We then discuss the various functionalities and controllability demonstrated by these micropumps, ending with a brief discussion of how they can be improved in the future. Due to the absence of external power sources, versatile activation methods and sensitivity to environmental cues, chemically powered micropumps could find potential applications in a wide range of lab-on-a-chip devices.

Received 10th January 2016,
Accepted 10th March 2016

DOI: 10.1039/c6lc00032k

www.rsc.org/loc

Introduction

Microfluidics is the science and technology of handling small amounts of fluids (10^{-9} to 10^{-18} liters) in small confinements such as microchannels[1] and can be applied in many fields such as protein crystallization,[2] separation in mass spectroscopy,[3] high-throughput screening,[4] molecule[5] and cell[6] manipulation, biochemical analysis,[7] drug delivery,[8] microchip

[a] *School of Materials Science and Engineering, Harbin Institute of Technology, Shenzhen Graduate School, Shenzhen, Guangdong 518055, China. E-mail: weiwang.psu@gmail.com*
[b] *Department of Chemistry, The Pennsylvania State University, University Park, PA 16802, USA*

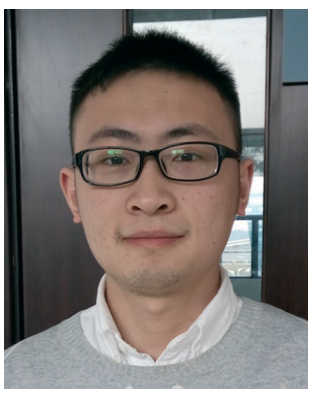

Chao Zhou

Chao Zhou received his bachelor's degree from Harbin Institute of Technology (Weihai) in 2013 and joined Prof. Wang's lab at Harbin Institute of Technology, Shenzhen Graduate School in 2014. He is currently a second year PhD candidate in the School of Materials Science and Technology, working on using chemistry to produce powered motion on the nano- and microscale. During his undergraduate research, Mr. Zhou simulated the flow in an artificial mesoporous network. His current research involves both experimental and numerical simulations.

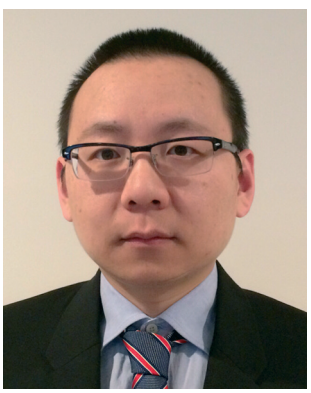

Hua Zhang

Hua Zhang was born in Zhengzhou, China. He obtained his bachelor's degree in Chemistry and master's degree in Polymer Chemistry and Physics at Wuhan University in 2005 and 2007, respectively. He then joined Dr. Ayusman Sen's lab in the Department of Chemistry of Pennsylvania State University in 2007, working on polymer-based micropump systems and antimicrobial polymers. After graduation, he started working for Lubrizol Corporation in Brecksville, Ohio as a R&D scientist. His current research interest is surface modification of thermal plastic polyurethanes for biomedical applications. Dr. Zhang has published or co-authored 12 peer-reviewed papers and 2 book chapters.

cooling[9] and chemical synthesis.[10] Lab-on-a-chip devices have recently emerged as a useful solution to integrating microfluidic systems in a single chip, greatly expanding the applicability of microfluidic technologies.[11] These devices can function as a complete laboratory on a single chip *via* tight integration of various micro-components including micropumps, channels, mixers, reservoirs, chambers, integrated electrodes, valves, sensors and so on,[11,12] greatly reducing the sample amount and time required to carry out sometimes rather sophisticated procedures.

Many of the useful applications as well as practical limitations of microfluidics involve microscale fluid flows, which are fundamentally different from macroscale hydrodynamics. For example, the Reynolds number, which is defined as the ratio of inertial forces over viscous forces, is typically very small in microfluidic environments, indicating that viscous forces dominate at such scales and flows are laminar in nature. Furthermore, diffusion plays a much more important role in the mass transport in microfluidic channels, as characterized by the Peclet number. High surface area-to-volume ratios and significant surface tension are also important issues in microfluidics that greatly increase hydrodynamic drag.[11,13] These properties inevitably lead to operational challenges in how to drive fluid flow in microchannels efficiently, conveniently and in a controllable fashion. On the other hand, the integration of numerous components in a small chip poses a major and fundamental challenge to the development of lab-on-a-chip devices. Pumps as a central component to power the fluid flow in such devices also need to be miniaturized. Innovative designs of micropumping systems that can address the above issues are therefore highly desired.

To date, micropumps of numerous types have been designed and fabricated, with different structures and operating mechanisms. As they are used in a wide range of applications, micropumps with different performances are required to satisfy different application scenarios.[14] For example, some are of small sizes and produce low hydraulic pressure, power and flow rates, while others are relatively large and operate at high pressure, power and flow rates. The most often used micropumps in microfluidic devices can be generally divided into two categories: (1) mechanical displacement pumps which apply forces to working fluids *via* moving boundaries between the solid and fluids or between different liquid phases and (2) electro- and magneto-kinetic pumps which provide energy to fluids continuously and as a result generate constant flow.[15] Some displacement micropumps (especially diaphragm pumps) are relatively mature,[15] and many of them can achieve high pressure and flow rates with very stable performance. However, the often relatively complex structures and the requirement of components such as valves for displacement micropumps pose a major challenge to their miniaturization and integration into lab-on-a-chip devices.

Electro- and magneto-kinetic micropumps include electrohydrodynamic, electroosmotic and magnetohydrodynamic pumps among others. Electrohydrodynamic pumps drive fluid flow through electrical forces acting on dielectric liquids, while charged fluid layers near a solid boundary move under an applied electric field in electroosmotic pumps.[16] Therefore, the pumping performance of these two types of pumps relies heavily on the electrical properties of the working fluids and the microchannel surface. These electrokinetic pumps, which are often unsuitable for macroscale uses, have advantages such as simple structures without moving parts, ease of fabrication and integration, and the ability to generate continuous and precise flow[15] with high pumping efficiency.[17] Yet, the requirement of external power sources adds an unwanted layer of complexity in the design of highly integrated lab-on-a-chip devices.

For lab-on-a-chip devices, the implementation of "self-supplied" compact micropumps has been proposed for PCR chips operating without a power supply.[18] In previous works, autonomous components such as chemical actuators and even autonomous microfluidic control based on the decomposition of H_2O_2 have also been reported.[19,20] Inspired by ubiquitous biological chemical pumps such as sodium–

Zeheng Li

Zeheng Li received his bachelor's degree from Harbin Institute of Technology (Weihai) in 2014 and joined Prof. Wang's lab at Harbin Institute of Technology, Shenzhen Graduate School. He is currently a second year master's degree student in the School of Materials Science and Technology. His current research is focused on synthetic microswimmers, particularly their behaviors in confined spaces.

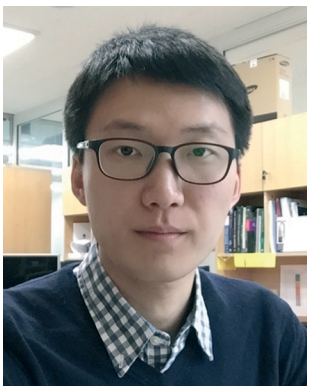

Wei Wang

Wei Wang graduated from Harbin Institute of Technology in 2008 with a bachelor's degree in Applied Chemistry. He then went to Pennsylvania State University (USA) where he pursued his PhD in Chemistry under the supervision of Prof. Thomas Mallouk. After obtaining his PhD, he returned to China in 2013, where he is currently an associate professor in the School of Materials Science and Technology at Harbin Institute of Technology, Shenzhen Graduate School. His research interests cover powered motion on the nano- and microscale, self-assembly and smart materials.

potassium pumps on cell membranes,[21] more self-powered chemical micropumps have been recently developed and can autonomously convert the chemical energy stored in the surrounding environment into fluid pumping.[22] Although they appear to be employing different mechanisms, these chemical pumps are in fact similar to traditional micropumps, which use a gradient of pressure or electromagnetic fields. Chemical pumps often take advantage of local gradients of solutes that result from a chemical reaction. However, compared with externally powered micropumps, self-powered chemical micropumps are distinct in terms of their ability to sense and respond to one or more external stimuli, simple structures, the lack of need for external control systems, ease of miniaturization, and the possibility to be integrated into microfluidic devices. These chemical micropumps therefore open up new and exciting avenues for manipulating flows in microfluidic devices, demonstrating great potential in the future development of lab-on-a-chip devices in areas such as

Table 1 Summary of the performance and features of various chemically powered micropumps

Operating mechanisms	Chemistry involved	Pumping velocity[a]	Estimated enthalpy change[b] (ΔH, kJ mol^{-1})	Notable features	Pump materials	Ref.
Self-electrophoresis and self-electroosmosis	Decomposition of H_2O_2	~17 μm s^{-1} (+40 mV tracer microspheres) in 0.5% H_2O_2	−196	Particle patterning	Ag and Au	26
	Decomposition of H_2O_2	10–20 μm s^{-1} (+46 mV tracer microspheres) near edge in 1% H_2O_2	−196	Particle patterning	Pt and Au	38
	Decomposition of H_2O_2	0.9 nL s^{-1} in 0.01% H_2O_2	−196	Mass transport acceleration	Pt and Au	39
	Decomposition of N_2H_4 ($N_2Me_2H_2$)	4 μm s^{-1} (−44 mV tracer microspheres)	−34 (N_2H_4)	Different fuels other than H_2O_2	Pd and Au	40
	Photoelectrochemical hydrolysis	7–12 μm s^{-1} (+46 mV tracer microspheres) near edge; speed increased to 45–70 μm s^{-1} in the presence of H_2O_2	571	Visible light-driven; biocompatibility	p-Type Si and Pt	41
Electrolyte self-diffusiophoresis	Photoelectrochemical hydrolysis	NA	571	UV light-driven; biocompatibility	TiO_2	47
	Dissolution of minerals in water	2–10 μm s^{-1} (−30 mV tracer microspheres)	−242	Only water is needed to initiate pumping; slow process; pump dissolves in the end	$CaCO_3$	50
	Decomposition of PAG-1	~7.2 μm s^{-1} (+55 mV tracer microspheres)	238	Stimuli-responsive; can be fabricated into colloidal photodiodes	PAG-1	51
	Decomposition of PFA-S	~3.2 μm s^{-1} (−140 mV tracer microspheres)	9		PFA-S	
Non-electrolyte self-diffusiophoresis	Depolymerization reactions	~1 μm s^{-1} in 0.06 M F^-	−745n–157 (n is the number of repeating units)	Stimuli-responsive; can transport particles in relatively long distances	TBS-PPHA	52
		~7 μm s^{-1} at pH 13	NA		PECA	
Density-driven	Host–guest reactions	1–4 μm s^{-1}	NA	Responsive to two stimuli; rechargeable	(β-CD-PEG) gel, *trans*-azobenzene	59
	Enzyme-based catalytic reactions	1–5 μm s^{-1}	−196	Stimuli-responsive; biocompatibility	Catalase	55
		0.3–0.5 μm s^{-1}	−29		Lipase	
		0.2–0.8 μm s^{-1}	−222		Glucose oxidase	
		0.2–0.8 μm s^{-1}	−34		Urease	
		1–1.5 μm s^{-1}	−63		DNA polymerase	58
	Transesterification reactions	~1.5 μm s^{-1} in 0.02 M glucose	−14	Stimuli-responsive; biocompatibility	Boronate ester	57
Bubble propulsion	Decomposition of H_2O_2	NA	−196	Low H_2O_2 concentration required; strong mixing effect	Pt	65, 66

[a] The velocities of tracers as well as fluids are influenced by the zeta potentials of the spheres and the charged substrate, "fuel" concentration and the location, and are only an indication of the order of magnitude of the pumping performance. [b] The enthalpy changes are estimated from the bond energy or standard molar formation enthalpy of the reactants and products.[35,36]

biology and medicine, analysis and detection, dynamic self-assembly of superstructures, drug delivery and so on.[23–25]

In this article, we review the recent progress in the design and fabrication of chemically powered micropumps, focusing on their structures, pumping mechanisms and functionalities (briefly summarized in Table 1). Although they differ in specific operation mechanisms, their activation always involves chemical reactions. In the conclusions section, we provide some perspectives on how these micropumps can be improved along with ideas for future development in this field. We hope that this review article, which is the first article entirely dedicated to this subject, serves as a starting point for researchers in microfluidics and related fields to learn the power of chemical reactions that can be harnessed for pumping.

Mechanism of chemical micropumps

Self-electrophoresis and self-electroosmosis

One of the earliest designs of self-powered micropumps is the bimetallic catalytic pumps.[26] Inspired by the previous gold–platinum (Au–Pt) bimetallic microrod motors that showed autonomous and directional motion in hydrogen peroxide (H_2O_2) solutions,[27] Kline *et al.* deposited silver rings and disks of 60–120 μm diameter on a gold surface (shown in Fig. 1B).[26] This gold–silver (Au–Ag) pump when immersed in dilute solutions of H_2O_2 could drive the fluid flow from the outside towards the center of the silver disk. In addition, electrically charged tracer microparticles could also be transported by such pumps and assembled into various patterns.

Similar to the bimetallic catalytic micromotors, the fluid pumping by catalytic micropumps is primarily driven by self-electrophoresis and is further complicated by self-electroosmosis (illustrated in Fig. 1A).[28] A bimetallic microrod made of metals that are active towards catalyzing the decomposition of H_2O_2 starts to move autonomously when suspended in H_2O_2 solutions. This was first discovered around the year 2004,[27] and was later attributed to a bipolar electrochemical reaction occurring on the surface of the metal rods.[28–31] It is important to revisit the mechanism responsible for such autonomous motion. For example, due to the different ability to catalyze the decomposition of H_2O_2 between Pt and Au, the oxidation of H_2O_2 on the surface of a Au–Pt microrod preferentially occurs at the Pt end (anode) where protons are produced in excess. Meanwhile, the reduction of H_2O_2 occurs preferentially at the Au end (cathode) and protons are consumed. The reactions are shown in eqn (1)–(3):

$$\text{Overall: } 2H_2O_2 \rightarrow 2H_2O + O_2 \quad (1)$$

$$\text{Anode: } H_2O_2 \rightarrow O_2 + 2H^+ + 2e^- \quad (2)$$

$$\text{Cathode: } H_2O_2 + 2H^+ + 2e^- \rightarrow 2H_2O \quad (3)$$

This bipolar reaction results in an asymmetric distribution of protons around the rod and consequently a distribution of space charges, which further leads to a self-generated electric field that points from Pt to the Au end. As a result, negatively charged Au–Pt microrods would move with the Pt end in a manner similar to regular electrophoresis.[32–34]

Bimetallic micropumps in H_2O_2 are driven by a similar mechanism. For example in the gold–silver (Au–Ag) micropumping system that Kline *et al.* developed (Fig. 1B), the silver disk serves as the cathode and the gold coating surrounding the silver disk serves as the anode. As a result, when the

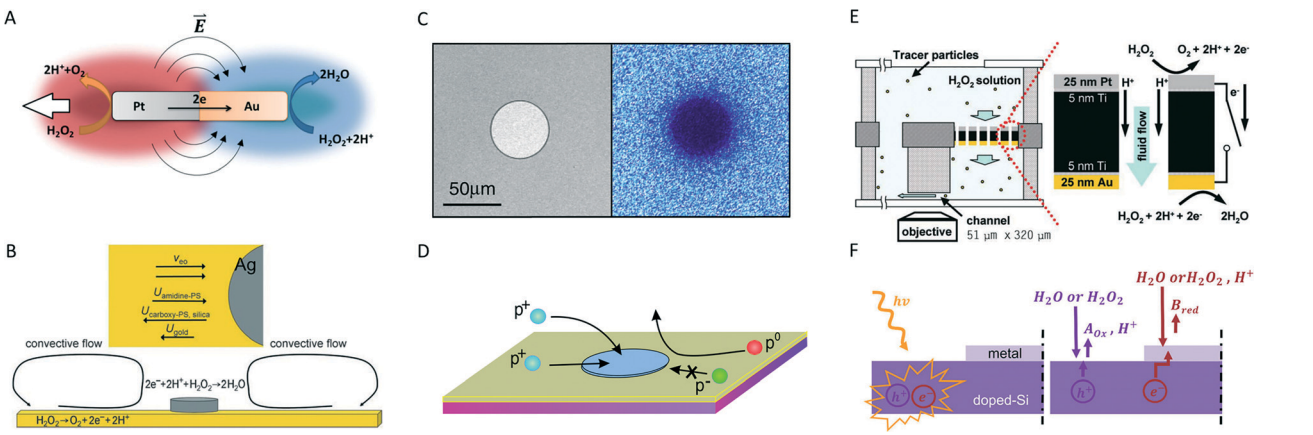

Fig. 1 (A) Scheme of a Au–Pt bimetallic microrod motor driven by the self-electrophoretic mechanism. Reprinted with permission from ref. 28, Copyright 2012 American Chemical Society. (B) Schematic diagram of a 3D convective flow and directions of the electroosmotic velocity of the fluid (V_{eo}) and electrophoretic velocities (U) of various tracer particles in a Au–Ag micropump. Adapted with permission from ref. 26, Copyright 2005 American Chemical Society. (C) Left: Confocal fluorescence microscopy image of a Au–Pt catalytic pump (Pt disk at the center); right: image of proton concentration (darker color corresponds to a lower proton concentration). Reprinted with permission from ref. 38, Copyright 2006 American Physical Society. (D) Schematic of the movement of differently charged tracer particles in the same Au–Pt catalytic pump as in (C) (p^+, p^- and p^0 correspond to positive, negative and neutral tracer particles, respectively). Reprinted with permission from ref. 38, Copyright 2006 American Physical Society. (E) Scheme of a self-pumping polycarbonate porous membrane deposited with Au and Pt on the two sides of the membrane in H_2O_2 solutions. Reprinted with permission from ref. 39, Copyright 2010 John Wiley and Sons. (F) Schematic of the proposed photoelectrochemical mechanism of light-driven silicon-metal pumps. Reprinted with permission from ref. 41, Copyright 2015 American Chemical Society.

bimetallic structure is exposed to H_2O_2 solution, an electric field that points from gold to silver (*i.e.* pointing inward to the center) emerges. However, unlike microrods that begin to move in this electric field, micropumps are fixed on a substrate and therefore remain stationary, thus pumping fluid. To elaborate on the pumping mechanism, the charged fluid layer in the electrical double layer next to the pump surface will flow along the surface under the effect of the electric field, a phenomenon known as electroosmosis. In the case of a Au–Ag micropump, the metal surface typically carries negative charges, and the fluid layer therefore carries positive charges. The surface fluid layer therefore moves in the same direction as the electric field, pointing inward from Au to Ag. This forms the basis of catalytic micropumps, where surface electrochemical reactions generate an electric field and drives charged fluid layers to flow on the pump surface. Due to fluid continuity, the fluid flows upward near the silver disk and outward on a layer at a certain distance above the bottom substrate. A 3D convective flow is then formed (see Fig. 1B).

Due to the presence of an electric field as well as the electroosmotic flow near the substrate surface, charged tracer particles near a catalytic micropump can move by two mechanisms: (1) electrophoretic motion of the particle under the direct effect of the electric field; (2) convective motion from the fluid drag of the electroosmotic flow. Therefore, the total particle velocity is the sum of the electroosmotic velocity (V_{eo}) and electrophoretic velocity (V_{ep}), which can be calculated from eqn (4) and (5), respectively:

$$V_{eo} = \frac{-\varepsilon\zeta_w E}{\eta} \quad (4)$$

$$V_{ep} = \frac{\varepsilon\zeta_p E}{\eta} \quad (5)$$

where ε is the permittivity of water, ζ_w is the zeta potential of the substrate, ζ_p is the zeta potential of the particle, η is the viscosity of the fluid and E is the electric field strength.

The electric field can be further obtained by solving the Nernst–Planck equation across the double layer, and the velocity of the charged tracer particle along the surface V_r can be calculated through eqn (6):[37]

$$V_r = \frac{\varepsilon(\zeta_p - \zeta_w)E_r}{\eta} \quad (6)$$

where E_r is the radial component of the electric field strength.

Farniya *et al.* further elucidated the operating mechanism of a Au–Pt catalytic pump by using fluorescence techniques to map the concentration of protons around the micropump.[38] To be more specific, dye molecules (pyranine) emit fluorescence signals of different intensities at different proton concentrations, enabling a direct correlation of the fluorescence intensity and proton concentration in the system by confocal microscopy. Their results show a higher proton concentration at the anode surface (gold substrate), which produces protons, and a lower proton concentration at the cathode surface (platinum disk), where protons are consumed (shown in Fig. 1C), providing the first visual evidence of the bipolar electrochemical mechanism.

In addition, by carefully tracking the transport of tracer particles of different surface charges near the pump (shown in Fig. 1D), the radial electric field generated by the electrochemical reactions on the pumps and the resulting electroosmotic fluid velocity are calculated, lending further support to the electrochemical mechanism.

Different from the above examples where bimetallic micropumps are constructed in a concentric fashion on a surface, Jun *et al.* built an operating chemical micropump out of a porous polycarbonate membrane by depositing Pt and Au on the opposite surfaces of the membrane which has microchannels through it.[39] Operating through the same bipolar electrochemical mechanism, the Pt and Au coatings act as the anode and cathode, respectively, in the presence of H_2O_2 when they are electrically connected (shown in Fig. 1E). The structure and functionality of this self-pumping membrane bears an interesting resemblance to active pumps on cell membranes,[21] and it can transport fluid and tracer particles from one side to the other at a flow rate of 0.9 nL s^{-1} and a pumping efficiency of 3 nL μA^{-1} s^{-1} in a very dilute H_2O_2 solution of 0.01 wt%. The performance can be potentially improved by increasing the fuel concentration.

In the above self-powered micropumping systems, H_2O_2 is often used as the fuel to drive the pumping. However, there has been ongoing research on replacing H_2O_2 with other chemicals. For example, Ibele *et al.* used hydrazine (N_2H_4) and *asym-N,N*-dimethylhydrazine ($N_2Me_2H_2$) as the fuel to drive gold–palladium (Au–Pd) catalytic pumps.[40] Their study on tracer particles also revealed two important facts about catalytic micropumps. First, for particles carrying charges of the same signs as the substrate, the electrophoretic motion and convective motion from electroosmosis always compete with each other (see eqn (4) and (5)), and the relative magnitude of ζ_p and ζ_w determines which effect dominates. Second, the exact electrochemical nature of the electrodes (*i.e.* whether a metal acts as a cathode or an anode) can be changed in different fuels. For example, for the Au–Pd pump discussed here, Pd acted as the anode in N_2H_4 solution, but as the cathode in $N_2Me_2H_2$. Although the authors successfully demonstrated that chemicals other than H_2O_2 could drive micropumps, hydrazine and its derivatives are still far from being ideal candidates which are often required to be environmentally friendly and/or biocompatible.

Light can also induce fluid pumping *via* electrochemical reactions, and this was demonstrated by Esplandiu and co-workers.[41] They reported a novel micropump based on semiconductor and metal materials operating under visible light in aqueous solutions (Fig. 1F). They deposited platinum disks of 30–50 μm in diameter and 50 nm in thickness on the top of p-type doped silicon and observed directional migration of tracer particles, indicating fluid flow. Although

not completely elucidated, a pumping mechanism based on electron–hole separation under visible light was proposed. To be more specific, electrons in the doped silicon were believed to be excited from the valence band to the conduction band by photons, while holes were also formed in the valence band at the same time. These electrons and holes then participated in the reductive and oxidative half reactions on the metal surface and silicon surface, respectively, and an overall hydrolysis reaction occurred. As a result of the spatial separation of the two half reactions, a concentration gradient of protons formed and led to an electric field that pointed from the silicon surface (anode) to the Pt surface (cathode), which consequently pumped fluid along with tracer particles. Although the generated electric field was relatively weak, these pumps could still perform effectively in water thanks to the abundance of negative charges on the surface of doped silicon (therefore strong electroosmosis). Besides, it was found that the pumping performance of these pumps could be enhanced with an increase in light intensity or in the presence of oxidizing agents such as H_2O_2. Although light has been previously used to drive micropumps,[42–44] this work represents the first example of achieving self-powered pumping on the microscale that takes advantage of photo-electrochemical reactions. Silicon-based pumping is especially attractive because it can be potentially integrated into many current designs of microfluidic devices, and the use of visible light further widens the applicability of this technique.

Self-diffusiophoresis

In the previous section, we have introduced a popular mechanism to induce fluid motion by chemical reactions and the resulting electric field. We now turn to a somewhat different mechanism that also generates a concentration gradient, but not necessarily an electric field. In this mechanism which is termed diffusiophoresis, the concentration gradient of solutes in the solution can cause fluid pumping.[33] Such a mechanism has been applied in a number of systems to produce self-propelled colloidal particles,[45–49] and as in the case of the electrophoretic mechanism, pumps emerge when the moving particles are immobilized.

In order to understand how diffusiophoretic pumps work, it is important to first understand how concentration gradients can cause particles or fluids to move (illustrated in Fig. 2). For a colloidal particle that releases electrolyte solutes, the solute molecules dissociate into cations and anions, which often diffuse at different rates. As a result, the space charge distributes unevenly in solution, and an electric field would form that points towards or away from the particle, depending on which charge species diffuse faster. The self-generated electric field then causes particle motion and inter-particle interactions. Such an electrical effect based on the different diffusivities of charged ions is referred to as the electrophoretic component of diffusiophoresis (Fig. 2 only illustrates this component). On the other hand, these differently charged ions also affect the double layer of the particle and induce a driving force along the ion gradient, and this is referred to as the chemophoretic effect. The overall diffusiophoresis is the total sum of these two effects, and the name *self-diffusiophoresis* indicates that the concentration gradient is produced by the particle itself. When a particle is close to a substrate, both the electrophoretic component and chemophoretic component act on the particle as well as the charged fluid layer immediately above the substrate. The velocity of particles exposed to a concentration gradient of electrolytes is given by eqn (7):[33]

$$V = \frac{\nabla C}{C_0}\left[\left(\frac{D^+ - D^-}{D^+ + D^-}\right)\left(\frac{k_B T}{e}\right)\frac{\varepsilon\left(\zeta_p - \zeta_w\right)}{\eta}\right] + \frac{\nabla C}{C_0}\left[\left(\frac{2\varepsilon k_B{}^2 T^2}{\eta e^2}\right)\left\{\ln\left(1-\gamma_w{}^2\right) - \ln\left(1-\gamma_p{}^2\right)\right\}\right] \quad (7)$$

where D^+ and D^- are the diffusion coefficients of the cation and anion, respectively, C_0 is the bulk concentration of ions, e is the charge of an electron, k_B is the Boltzmann constant, T is the absolute temperature, ε is the dielectric permittivity

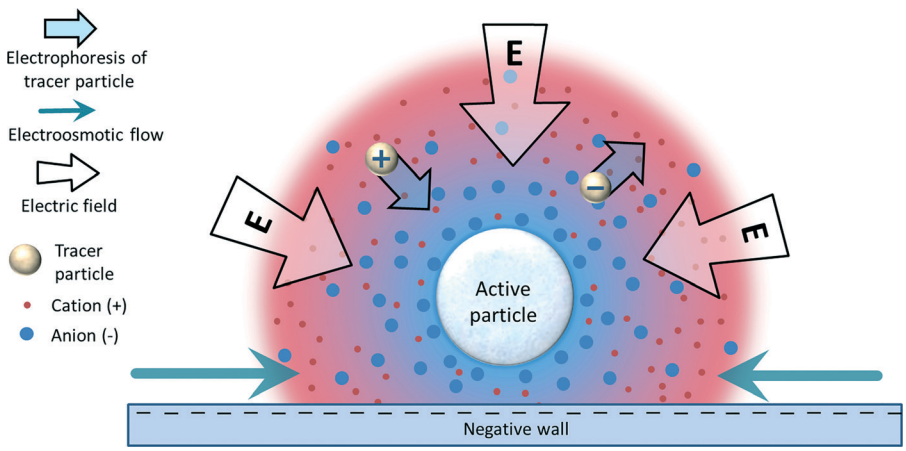

Fig. 2 Scheme of electrolyte diffusiophoresis near a negatively charged substrate.

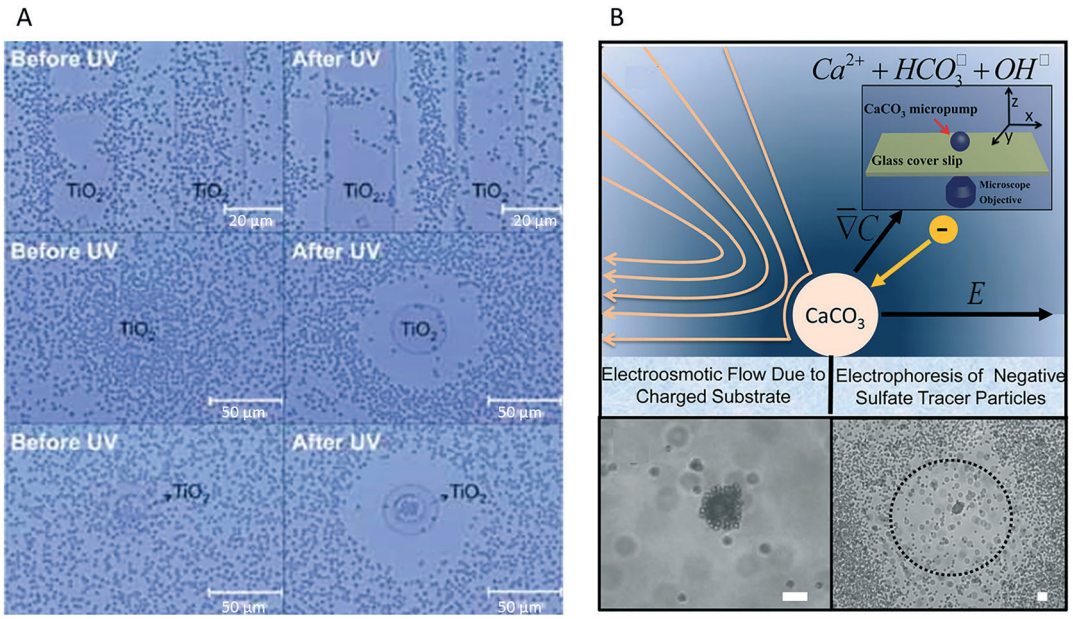

Fig. 3 (A) Various designs of TiO_2 micropumps and the patterns of tracer particles. Adapted with permission from ref. 47, Copyright 2010 John Wiley and Sons. (B) Schematic of electroosmotic flow and electrophoresis of negatively charged tracers near the $CaCO_3$ particle micropump (top) and optical microscopy images of negatively charged tracer particles around the micropump (bottom). Reprinted with permission from ref. 50, Copyright 2010 American Chemical Society. Scale bars are 10 μm.

of the solution, η is the viscosity, ζ_p and ζ_w are the zeta potentials of the particle and wall, respectively, and $\gamma_w = \tanh(e\zeta_w/4k_BT)$, $\gamma_p = \tanh(e\zeta_p/4k_BT)$. The first part of eqn (10) represents the electrophoretic component, and the second part represents the chemophoretic component. It is easy to imagine that once the active particle is fixed on the substrate, it becomes a diffusiophoretically active micropump, inducing fluid flow and attracting/repelling nearby charged particles.

A pioneering example of micropumps operating by diffusiophoresis was developed by Hong *et al.* by taking advantage of the photonic properties of titanium oxide (TiO_2) microparticles.[47] Under ultraviolet light, electrons are excited into the conduction band in TiO_2, and the produced electron–hole pairs reduce and oxidize water molecules in water, respectively. This is very similar to the Si–Pt micropump discussed in the previous section, except that in the case of the Si–Pt micropump, the proton concentration gradient along the cathode and anode generates electroosmotic pumping. In this case, however, TiO_2 films produced superoxide ions (O^{2-}), hydroxyl radicals ($^{\bullet}OH$), hydroxyl ions (OH^-) and protons. These ionic products diffuse at different speeds, resulting in a local concentration gradient of charged species and a self-generated electric field around the TiO_2 particles based on the self-diffusiophoretic mechanism. Based on such principles, Hong *et al.* fixed TiO_2 thin films of different shapes on a glass substrate, which when irradiated with UV light could pump the fluid away from the TiO_2 layers (shown in Fig. 3A). The major advantages of this self-diffusiophoretic system are the absence of toxic chemicals involved in the operation of the pumps (such as H_2O_2 or N_2H_4), as well as the high level of controllability by light intensity and on–off switch. However, the main issue that limits the use of TiO_2 micropumps in potential biomedical applications is their inability to operate at high ionic strength, since diffusiophoresis is inherently very sensitive to the presence of ions.

Diffusiophoretic micropumps made of materials other than TiO_2, including both inorganic and organic materials, have been subsequently developed. For example, spherical particles of calcium carbonate ($CaCO_3$) of 10 μm diameter were fixed on a substrate and the movement of tracer particles was observed in aqueous solution by McDermott and coworkers.[50] Although hardly soluble, $CaCO_3$ molecules on the particle surface slowly dissolved in the unsaturated solution. The dissociated ions (Ca^{2+}, HCO_3^- and OH^- ions) had different diffusion coefficients leading to diffusiophoretic pumping of the fluid near the substrate. Fig. 3B illustrates the motion of negatively charged sulfate-functionalized polystyrene latex microsphere particles (sPSL) and the electroosmotic flow near a $CaCO_3$ pump. Barium carbonate ($BaCO_3$) microparticles can also pump fluids and tracer particles in a similar manner but with more power, because of the larger difference in the diffusion coefficients between Ba^{2+} and OH^-. This type of pump is distinct in that the pump operates on the natural dissolving process of rock materials, which eventually disappears in flowing water and stops the pumping. Two clear drawbacks emerge: (1) the dissolving process is relatively uncontrolled and it is therefore difficult to manipulate pumping externally; (2) the cations released (*e.g.* Ba^{2+} and Ca^{2+}) can easily adsorb on the surfaces of substrates and nearby particles, altering their zeta potential and leading to more dynamic and complicated pumping performance.

Organic molecules such photoacid generator (PAG) *N*-hydroxyphthalimide triflate (referred to as PAG-1) and poly(4-formylphenyl acrylate) aniline Schiff base (PFA-S) were

also used by Yadav and co-workers to make self-powered micropumps based on the self-diffusiophoretic mechanism.[51] PAG-1 decomposed into *N*-hydroxyphthalimide, protons and triflate anions under 365 nm UV light as shown in Fig. 4A. The positively charged protons diffused faster than the negatively charged triflate anions, generating an electric field pointing towards the polymer piece (pump). Electroosmosis on the charged substrate ensues. PFA-S, on the other hand, underwent a decomposition reaction in the presence of HCl as shown in Fig. 4B and produced chloride anions and organic cations. Since the anions were much smaller in size, they diffused much faster than the cations, and the electric field direction as well as the pumping direction was therefore opposite to PAG-1 pumps.

A concentration gradient of neutral species can also cause diffusiophoretic movement and therefore induce pumping, and this is called non-electrolyte diffusiophoresis. In this case, the interaction between neutral solutes and the particle surface produces a pressure difference along the particle surface and consequently drives the particles and fluid. For example, Zhang *et al.* reported micropumps made of polymer films based on analyte-initiated depolymerization reactions. In their experiments, a piece of *tert*-butyldimethylsilyl (TBS) end-capped poly(phthalaldehyde) (TBS-PPHA) polymer film which is insoluble in water was attached to a glass substrate.[52] The polymer depolymerized into soluble monomers in response to chemical signals such as fluoride ions as shown in Fig. 4C. Poly(ethyl cyanoacrylate) (PECA) films can undergo similar reactions in the presence of hydroxyl ions (also in Fig. 4C). The concentration gradient of the produced monomers in both reactions can drive the tracer particles and fluid based on the non-electrolyte diffusiophoretic mechanism. These analyte-responsive self-powered micropumps can respond to specific chemicals, and the magnitude of the produced flow or particle motion is sensitive to the concentration of analytes, which shows promise for sensing applications. For example, the authors of this study combined detection agents with the pump to sense specific biomarkers. This is further discussed in Applications of self-powered chemical micropumps.

Density-driven pumps

Density-driven convective flow can also be employed by micropumps to drive tracer particles and fluids. Such flow is a result of an inhomogeneous distribution of local fluid density, which can be caused by thermal convection from exothermic reactions, concentration gradients of reaction products and other effects. In particular, a few self-powered enzyme-based micropumps have been developed based on the density-driven mechanism, especially for those that do not involve charged species. In these systems, the enzyme-functionalized pump is turned "on" when the enzyme molecules are exposed to their corresponding substrates. Fast enzymatic overturn of the catalytic reactions leads to significant density differences in the surrounding fluid that cause fluid flow, the magnitude of which is often tied to the concentration of the substrate, the overturn rate of the enzymatic reaction, as well as the enzyme coverage on the pumps.

Enzyme-based micropumps inspired by enzyme-powered nanomotors[53,54] typically have better biocompatibility than the previously discussed micropumps and can sense and respond to specific biologically relevant analytes such as

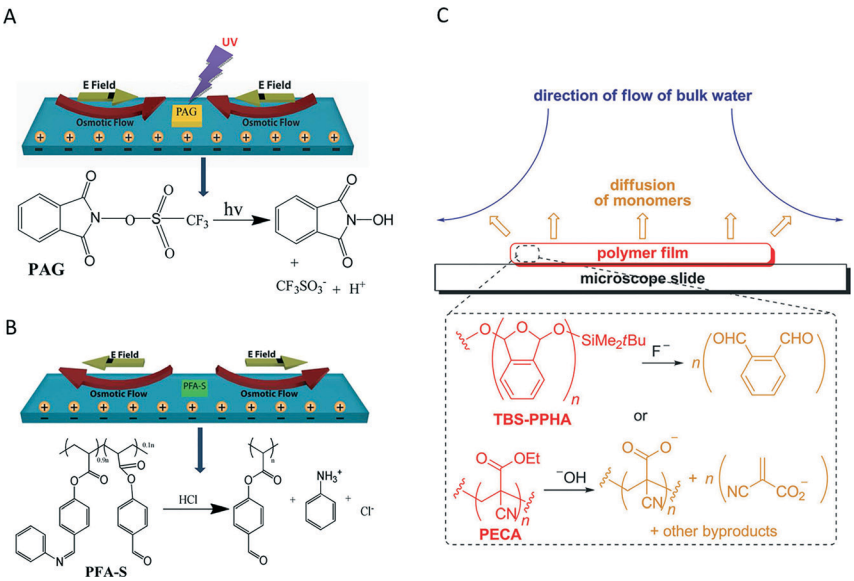

Fig. 4 (A) Schematic depiction of a chemical pump made of PAG (*N*-hydroxyphthalimide triflate) and the corresponding decomposition reaction under UV light. (B) Schematic depiction of the PFA-S (poly(4-formylphenyl acrylate) aniline Schiff base)-based pump and the corresponding chemical reaction. (A) and (B) are reprinted with permission from ref. 51, Copyright 2012 American Chemical Society. (C) Schematic depiction of the operating mechanism of a pump based on analyte-initiated depolymerization reactions. Reprinted with permission from ref. 52, Copyright 2012 John Wiley and Sons.

substrates, promoters and biomarkers in living organisms. In a pioneering study, Sengupta *et al.* designed four kinds of enzyme-based micropumps using catalase, urease, lipase and glucose oxidase.[55] Fig. 5A presents a schematic of the assembly process and the function of these enzyme-based micropumps. The enzymes were patterned on the self-assembled monolayer (SAM)-modified Au surface by electrostatic self-assembly. In the presence of the corresponding substrates, the immobilized enzyme can pump nearby fluid and tracer particles. The authors noted an increase in the pumping velocity as the concentration of substrates and reaction rates were increased. Temporal and spatial changes of fluid-pumping velocity were also studied, and it was found that the pumping velocity decreased farther away from the pump and with the passage of time. Doubling the height of the experiment chamber, however, increased the pumping velocity by about 7-fold. In addition, as shown in Fig. 5A, adding glucose and glucose oxidase simultaneously to the catalase pump started the pump due to H_2O_2 produced, which demonstrated the pump's ability to sense more analytes than the corresponding substrate indirectly by carefully designing the enzymatic reactions on the pump surface.

During the early phases of the discovery of enzymatic micropumps, there was a controversy as to whether such pumps were driven by diffusiophoresis, thermal gradients or other mechanisms. In order to elucidate the working mechanism of these enzyme-based micropumps, the observation chamber of a catalase-driven pump which decomposed H_2O_2 into electrically neutral H_2O and O_2 molecules was inverted. It was found that the pumping direction completely reversed, lending strong support to gravity-based pumping mechanisms. Diffusiophoresis (either electrolyte or non-electrolyte type) can therefore be eliminated as the major pumping mechanism, since it would predict the same fluid flow direction for both configurations, considering that the direction of the concentration gradient would not change either way. The authors instead proposed a pumping mechanism based on fluid density differences around the pump. More specifically, they argued that the exothermic catalytic reactions by the catalase, lipase and glucose oxidase enzymes in the presence of their corresponding substrates increased the local

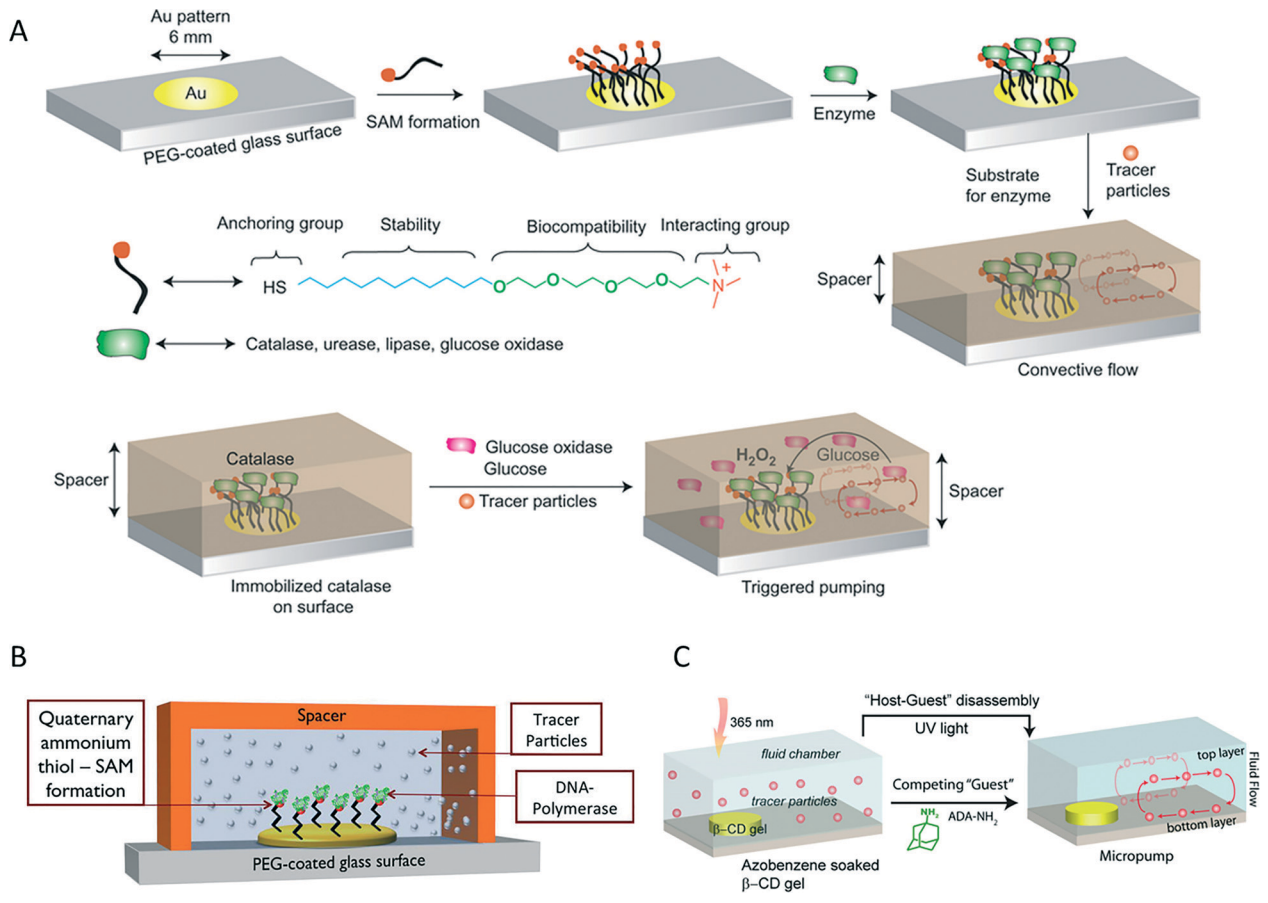

Fig. 5 (A) The fabrication process of an enzyme-functionalized micropump and an illustration of how catalase enzyme-based pumps are turned on in the presence of both glucose oxidase and glucose. Reprinted with permission from ref. 55, Copyright 2014 Nature Publishing Group. (B) Structure and schematic of a DNA polymerase-powered micropump. Reprinted with permission from ref. 58, Copyright 2014 American Chemical Society. (C) Structure and pumping schematic of dual stimuli-responsive micropumps based on "host–guest" interactions. Reprinted with permission from ref. 59, Copyright 2013 American Chemical Society.

temperature at the pump surface, which in turn lowered the fluid density near the pump surface. Therefore, when the pump was in the "facing-up" configuration, the fluid near the pump surface moved up due to buoyancy and the fluid around the pump would flow *inward* according to fluid continuity. When the pump was inverted, the buoyancy would cause the fluid near the pump surface to flow *outward* instead. Urease pumps were somewhat different in that although the enzymatic reaction was also exothermic, it pumped the fluid in the direction opposite to the above enzyme pumps in the "facing up" mode. This unexpected behavior was explored in detail in a very recent article by Ortiz-Rivera *et al.*, in which such pumping was found to be spatiotemporally dynamic, and a combination of theory and experiments was used to clarify the density-based mechanism.[56] In another experiment, it is shown that the transesterification of the boronate ester of *cis*-diols with glucose can also be harnessed in the design of glucose-driven micropumps.[57] The heat generated from the transesterification reaction changes the local density and causes the fluid to move in a manner similar to the previous pumps. Although this mechanism might be qualitatively reasonable, more quantitative analysis or actual measurement of the local density change would greatly facilitate the elucidation of the reason why different enzyme-based pumps operate in opposite directions, and whether there is any interplay between density-based and gradient-based mechanisms.

Local pumping by density change can be activated by means other than heat, as was demonstrated by Sengupta *et al.* in another experiment with pumps driven by DNA polymerase.[58] Similar to the above enzyme-based micropumps, DNA polymerase which could form a complex with the DNA template was attached to an Au surface functionalized with a quaternary ammonium thiol monolayer. The Au disk was deposited on a PEG-coated glass slide and the whole pump was packaged in a silicone spacer (shown in Fig. 5B). When nucleotide 2′-adenosine triphosphate (dATP) and cofactor Mg^{2+} ions were added to the system, the nucleotide would incorporate into DNA chains according to the previous DNA template. The pump was turned on and drove the fluid near the substrates inward to the gold surface. The pumping direction was also reversed when the chamber was turned upside down, ruling out phoretic mechanisms and indicating a density-driven mechanism by the same arguments as those in the previous study. However, the authors decided that the density difference was not caused by the same heat-induced fluid density inhomogeneity. In particular, although the catalytic reaction by DNA polymerase was exothermic, simulation showed that a power of 10^{-4} W was required to drive 1 μm s^{-1} fluid flow if thermal convection was entirely responsible for the fluid flow, while only a power of 10^{-9} W could be provided by the chemical reaction. Alternatively, the author argued that the local fluid density inhomogeneity was a result of two possible effects: (1) the change in the shape of the polymerase molecules which may influence nearby water molecules and reduce the local density; (2) the conversion of dATP into dAMP and PPi (pyrophosphate), which is required by the polymerase, may decrease the fluid density near the pump surface.

Based on similar principles and structures, Patra *et al.* designed micropumps with more functionalities.[59] They reported a rechargeable micropump that could respond to chemical and physical stimuli based on "host–guest" interactions. This pump can be considered as a "soft pump" because of the use of gel as the scaffold. Fig. 5C illustrates the structure and the fluid flow driven under two stimuli. A β-cyclodextrin polyethylene glycol (β-CD-PEG) gel soaked in *trans*-azobenzene solution was fixed on a substrate and packaged in an observation chamber filled with water and tracer particles. In this pump, β-CD-PEG was the guest and *trans*-azobenzene was the host, and the host–guest structure was formed in the soaking process. However, under UV light, *trans*-azobenzene underwent photochemical isomerization to *cis*-azobenzene of a weaker binding affinity, and the host–guest structure disassembled. Experimentally, this led to inward pumping of tracer particles near the substrate towards the pump under UV light.

Two possible pumping mechanisms were proposed by the authors. One was that the products of the host–guest disassembly reaction (*cis*-azobenzene) reduced the local density of the fluid and drove the fluid flow, similar to the above enzyme-powered micropumps. Alternatively, the host–guest disassembly reaction under UV light resulted in the release of guest molecules from the β-CD cavity, which was accompanied by water molecules entering the cavity. This process could induce an inward fluid flux. Besides being actuated by UV light, this pump can also respond to chemicals. For example, in the presence of 1-adamantylamine hydrochloride (ADA-NH_2·HCl) that has higher binding affinity to the β-CD guest than *trans*-azobenzene, the original β-CD–*trans*-azobenzene host–guest assembly structure disassembled and the reaction between β-CD and ADA-NH_2·HCl formed a new assembly structure. Such disassembly and reassembly processes also induced a local fluid density change and consequently pumped fluids. Another special feature of this pump is its rechargeability. Regardless of the exact mechanism, the pump operates only when the host–guest structure undergoes disassembly, and would stop pumping when all *trans*-azobenzene molecules leave the β-CD cavity. However, the pump can be "recharged" upon exposure to visible light where the released *cis*-azobenzene molecules isomerize back to *trans*-azobenzene and resume the original host–guest structure. After washing and repackaging with fresh solution, the recharged pump showed only a slight decline in performance.

Bubble propulsion

Similar to jet planes and rockets that are propelled by the thrust of exhaust, bubbles expelled by microscale objects can also push particles forward *via* momentum transfer. Such a process, often referred to as "bubble propulsion", has recently

been exploited in a wide range of self-propelled colloidal particles.[60–63] This mechanism can also induce fluid pumping when the bubble-generating part is fixed. In these bubble-driven micropumping systems, oxygen bubbles are often released from the catalytic decomposition of H_2O_2. For example, oxygen bubbles have been used for pumping fluids in lab-on-a-chip devices by the decomposition of H_2O_2 catalyzed by MnO_2.[20,64] More recently, inspired by their previous work on microtubular jet engines propelled by bubble recoiling,[60] Solovev *et al.* designed a tubular micropump roughly 100 μm in size that operated at a low concentration (0.06% v/v) of H_2O_2.[65] They rolled up Ti/Cr/Pt nanomembranes into conical tubes with Pt as the inner layer and fixed them on a substrate. In the presence of H_2O_2 solution, the inner Pt layer catalyzed the decomposition reaction of H_2O_2 and produced oxygen bubbles, which quickly grew in size and eventually were expelled from the larger opening of the tube. As the bubble grew and moved inside the tube, water was ushered in from the other opening of the tube, leading to a unidirectional fluid flow. In addition, tracer particles smaller than the tube opening can be sucked into the tube and transported from one end of the tube to the other (shown in Fig. 6). The H_2O_2 concentration and the size of the micropump were both found to influence the pump performance. For example, pumping was more intense at higher H_2O_2 concentrations, which reflects the higher reaction rate and higher bubble expulsion rate at higher H_2O_2 concentrations. However, when the concentration of H_2O_2 exceeded a certain threshold, the pump was "overloaded", which means that bubbles were released from both ends of the tube and the fluid no longer flowed unidirectionally. Longer tubes also acted as more sensitive pumps (lower H_2O_2 concentration needed to start the pump) because of larger surface areas of Pt. Similarly, Soler *et al.* reported microtubes that cleaned polluted water by the Fenton oxidation process.[66] The bubbles released from the tubes pumped the nearby fluid, and the convection enhanced mass transport of the contaminants and facilitated cleaning. Because of the compatibility of its fabrication methods with current microfluidic technologies and high pumping speeds, bubble-driven micropumps made of rolled up microtubes are potentially useful in applications such as particle sorting (by tube opening sizes), microreactors (both the inner and outer surfaces of the tube can be easily functionalized), and more.

Control of self-powered chemical micropumps

The controllability of self-powered micropumps, such as on/off switch and the velocity or directions of fluid flow, is an important factor to consider for practical applications. Much effort has been spent on building proof-of-concept systems that are capable of achieving these goals.

One way to design self-powered micropumps that can be switched on or off is through hardware designs. One of such examples was discussed in detail in the section on self-electrophoresis, where a micropump was made by depositing Pt and Au metals on the opposite sides of a polycarbonate membrane with nanopores (Fig. 1B). When the membrane is exposed to hydrogen peroxide solution and the two metal-coated sides are connected electrically, the oxidation and reduction of H_2O_2 preferentially occur at the Pt and Au ends, respectively, leading to an electroosmotic fluid flow within the nanopores from the Pt-coated side to the Au-coated side. This pump can be easily turned off by disconnecting the electrical contact. Stopping the pumping by disabling electrical connections is particularly useful for reactions that are electrical in nature, such as pumps that operate by self-electrophoresis.

For some micropumps, the chemical reactions that drive the pumps initiate only when specific stimuli such as UV light and specific analytes are present, and by providing or removing these external cues, the pumps can be turned on or off. For example, UV light is essential for the photolysis of TiO_2,[47] the degradation reaction of PAG[51] and the host–guest

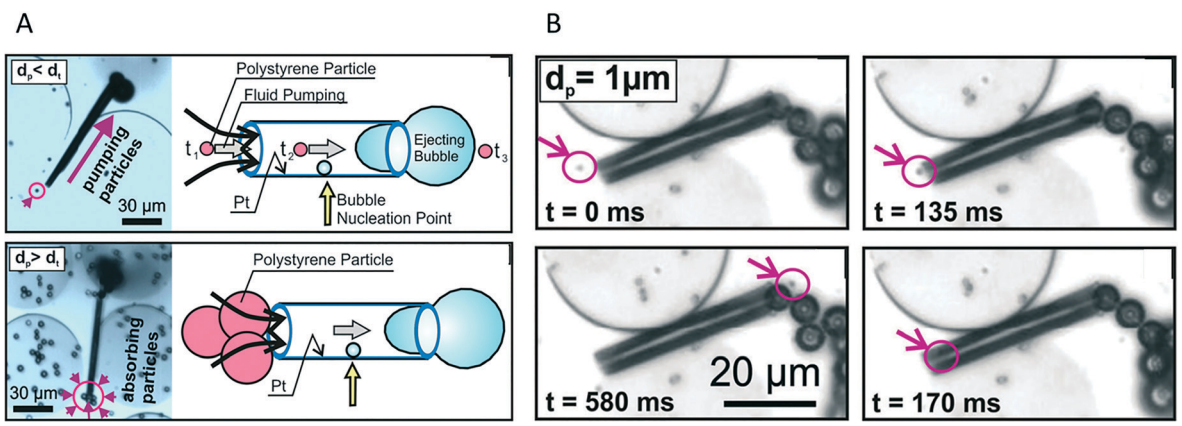

Fig. 6 (A) Optical microscopy images and sketches of Ti/Cr/Pt microtubes pumping polystyrene particles in H_2O_2. (B) Optical images of tracer particles being transported inside the tube. (A) and (B) are reprinted with permission from ref. 65, Copyright 2011 Royal Society of Chemistry.

disassembly between β-CD and *trans*-azobenzene[59] (discussed in Mechanism of chemical micropumps). These pumps therefore are turned on under UV light and off when UV light is removed. As far as chemical switches are concerned, micropumps driven by *trans*-azobenzene–β-CD host–guest reactions,[59] micropumps made of TBS-PPHA and those made of PECA[52] can respond to ADA-NH_2·HCl, fluoride ions and hydroxyl ions, respectively. When these analytes are present in the solution, the corresponding chemical reactions turn on the pump and induce fluid flows. Further, pumps based on host–guest reactions can respond to both chemical and physical signals. UV light and competing guests such as ADA-NH_2·HCl can both disassemble the original β-CD–*trans*-azobenzene assembly structure and in doing so start the pumps.[59] Such a response to more than one type of stimuli can be potentially exploited in the design of more complicated micropumps that have embedded logic gate functions, similar to swarms of Ag_3PO_4 microparticles that respond to both ammonia and UV light.[67] One benefit of using external cues such as UV light is its fast response; pumps are often immediately turned on or off when the light conditions change.

The pumping velocity of most chemical micropumps can be adjusted by varying the quantity or magnitude of stimuli, such as the concentration of "fuels" in diffusiophoretically or electrophoretically driven pumps, substrate concentrations or enzyme coverage in enzyme-powered pumps, and light intensity in UV-activated pumps. In addition, the size of the microtubular pump in particular was demonstrated to greatly affect the pumping performance,[65] as was discussed in the previous section. How sizes affect the pumping behaviors of micropumps powered by chemical reactions or light has remained largely unanswered. Intuition suggests that a larger pump surface means a higher total flux and could lead to a larger density change near the pump or a larger difference in the concentration of chemical species, depending on which mechanism is in operation. On the other hand, many pumps discussed in this article rely on some sort of gradient, which is inversely proportional to distance. Therefore, larger pumps do not necessarily pump faster, and more thorough and systematic studies are required to address this issue properly.

Applications of self-powered chemical micropumps

Self-powered micropumps can be applied in many areas, one of which is controlled drug delivery. One way is to use the fluid flow induced by the pump to convectively release molecules pre-embedded in the pump. For example, Sengupta *et al.* used positively charged hydrogels as scaffolds and fixed urease enzymes on the cross-linked scaffolds through electrostatic assembly (Fig. 7A).[55] Fluorescein dyes representing cargos were stored in the gel. When the substrate (urea) concentration increased, the enzymatic reaction turned the pump on, and the fluorescein dyes were released more quickly into the solution as the fluid was pumped than solely by diffusion. Furthermore, the authors also demonstrated the autonomous release of insulin by a glucose oxidase micropump at a physiologically relevant concentration of glucose (0.005 M). A similar proof-of-concept glucose-responsive micropump was designed by Zhang *et al.* based on the transesterification of the boronate ester of *cis*-diols with glucose using fluorescein dye.[57] These biocompatible and effective micropumps represent remarkable progress in the design of self-powered and intelligent drug delivery systems. We can imagine them being applied in scenarios where biological signals inherent to human bodies (such as pH, temperature, blood sugar level, oxygen concentration, *etc.*) can turn on (and possibly off) embedded devices to carry out biomedical operations.

Chemical micropumps can also transport microparticles in a controlled fashion. As discussed previously, *N*-hydroxyphthalimide triflate (PAG-1) micropumps produce *N*-hydroxyphthalimide, protons and triflate anions under UV light. Interestingly, the acidic product from the PAG-1 pump could also participate as a reactant in the decomposition reaction of poly(4-formylphenyl acrylate) aniline Schiff base (PFA-S), and consequently start the second micropump. By cleverly putting these two pumps next to each other, Yadav *et al.* fabricated a colloidal photodiode device where negatively charged tracer particles were pushed away from the PAG pump and pulled toward the PFA-S pump (Fig. 7B).[51] In such a case, the PAG pump effectively acted as a source and the PFA-S pump as a drain, resulting in the directional transport of the tracers from the PAG to the PFA-S pump. In another experiment, Zhang *et al.* demonstrated that in the presence of fluoride ions, *tert*-butyldimethylsilyl (TBS) end-capped poly(phthalaldehyde) (TBS-PPHA) pumps could transport particles over a distance of more than 5 mm and even around corners in a microfluidic channel (shown in Fig. 7C).[52] In the presence of fluoride, the TBS-PPHA pump at one end of the microchannel produced a high concentration of monomers and pumped the particles in the channel along the concentration gradient *via* non-electrolyte self-diffusiophoresis. More sophisticated designs and configurations of micropumps can in principle guide particles to move in a complicated microfluidic channel network in a path that is predetermined and programmable. But perhaps more interestingly, by selectively turning on and off specific pumping *via* stimuli as discussed above, cargos can be potentially transported in a dynamic and adjustable fashion in real time. The prospect of using chemical agents or external cues such as light, sound and electromagnetic fields to guide the flow of fluids and/or particles in the fluid *via* chemical micropumps is a promising technique that at least runs parallel to some existing methods such as externally operated microvalves.

A few studies of chemically powered micropumps operating by electrophoresis or diffusiophoresis showed that colloidal particles could assemble into organized structures near pumps. In some early studies of chemically driven

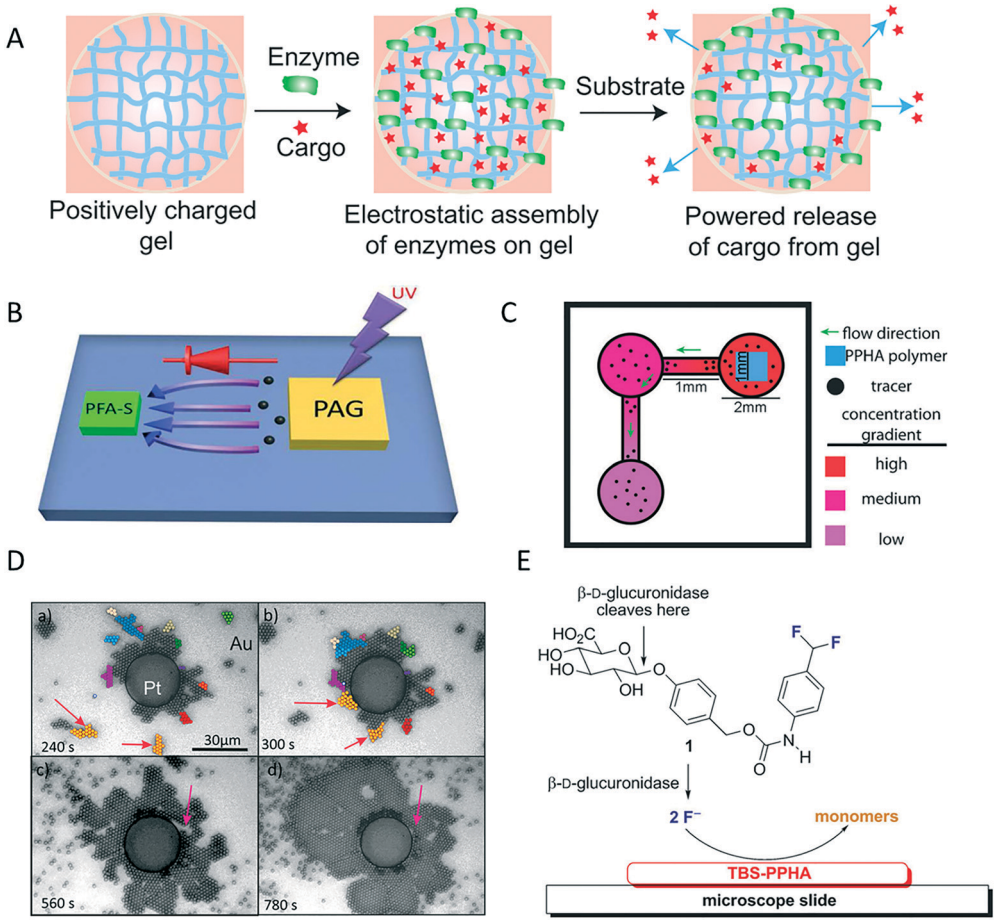

Fig. 7 (A) Schematic of the process of cargo release from enzyme-powered gel micropumps in the presence of substrate molecules. Reprinted with permission from ref. 55, Copyright 2014 Nature Publishing Group. (B) Schematic of a colloidal photodiode made of a combination of PAG as the source and PFA-S as the drain. Reprinted with permission from ref. 51, Copyright 2012 American Chemical Society. (C) Schematic of the TBS-PPHA pump that transports particles in a microchannel. (D) Healing process of defects in a colloidal crystal assembled by a Pt–Au pump. Reprinted with permission from ref. 68, Copyright 2014 American Chemical Society. (E) The β-D-glucuronidase enzyme turns "on" a TBS-PPHA pump in the presence of reagent **1**. (C) and (E) are reprinted with permission from ref. 52, Copyright 2012 John Wiley and Sons.

micropumps, it is often observed that tracer particles migrate towards the pump at the center, but once close to the center, they always remained at a certain distance away from the pump. Such an effect, referred to as the "exclusion zone", was often attributed to a competition between the electrophoretic migration of the tracer particles in the generated electric field and the electroosmotic fluid pumping which might be moving in the opposite direction.[47,48] Farniya *et al.* further studied this effect in disc-shaped Pt–Au catalytic micropumps (Pt at the center of a Au surface) and used it to direct the crystallization of colloids (Fig. 7D).[68] Interestingly, defects in the crystalline structure could be healed by the dynamic and spontaneous rearrangement of particles under fluid flows.

Due to their ability to respond to external chemical signals, self-powered chemical micropumps can also be applied in sensing applications. For example, the combination of a *tert*-butyldimethylsilyl (TBS) end-capped poly(phthalaldehyde) (TBS-PPHA) pump and detection reagent **1** whose structure is shown in Fig. 7E can be used to detect the presence of the β-D-glucuronidase enzyme (a specific marker of *E. coli*).[52] The reaction between the reagent and enzyme can release fluoride ions that turn on the TBS-PPHA pump, and the concentration of the enzyme can be determined by measuring the pumping velocity. For instance, the pumping velocity was about 1.3 μm s^{-1} in 3.1 mM β-D-glucuronidase solution. Other analytes can also be sensed by pumps working by the same principle if engineered with proper chemistry.

Conclusions and perspectives

Over the past few years, self-powered chemical micropumps have seen fast development. They can now be fabricated with a wide variety of materials (noble metals, polymers, mineral salts, metal oxides and enzymes) and can be powered by a number of innovative mechanisms that are particularly useful on the microscale (the ones of chemical nature are reviewed here). Besides being self-powered and able to pump fluids, each of these micropumps has its unique features including particle patterning, analyte sensing, rechargeability, response to dual stimuli, biocompatibility and more, which

render these pumps powerful in areas that might be inaccessible to macro-scale pumps. Proof-of-concept experiments, such as transport and release of drug molecules, directional and long-distance transport particles, and sensing of analytes, hint at the future prospects of chemical micropumps in the development of microscale smart devices.

Although much effort has been dedicated to improving the performance of chemical micropumps, it is important to acknowledge a number of issues that limit their practical uses. First, the energy conversion efficiency of chemically powered micropumps is still quite low, and the low pumping velocity cannot remain stable for an extended period of time either. This is probably the most serious issue that needs to be properly addressed before the micropumps reviewed here can be truly used in actual devices. Eventually, efficient micropumps that can produce fast and reliably stable fluid flow need to be developed. Second, selective patterning of a specific part of the surface is often required in the fabrication process of self-powered micropumps, and the associated difficulty in integrating this step into the overall fabrication of microfluidic channels might limit the wide application of micropumps in complex and integrated lab-on-a-chip systems, where many of the potential applications ultimately lie. Finally, many of the previously discussed pumps require specific (and often toxic) chemicals as either the pump materials or the chemical fuel that drive pumping, which are inevitably in contact with the flowing media. This may cause compatibility issues with many applications that are sensitive to the environment, especially those related to biological scenarios. Additionally, micropumps driven by electrophoresis or diffusiophoresis might not function properly at high ionic strength, prohibiting their application with many biologically relevant fluids. Therefore, achieving good compatibility without compromising the pumping performance remains a major challenge.

We expect to see chemically powered micropumps with novel designs that can address the above issues emerge in the coming years. The efficiency of micropumps could be greatly improved once we gain a deeper understanding of their working mechanism. On the other hand, by carefully engineering the micropump designs and possibly relaying many pumps together, continuous and steady pumping at a large spatial and temporal scope can also be achieved. Although faced with challenges, we should not overlook the unique advantages of many of these chemically powered pumps, including their versatility, diverse activation methods, ability to be designed into complicated systems and sensitivity to the chemical environment among others. The usefulness of these micropumps depends not only on their future development and improvement, but also very heavily on the particular scenario in which a micropump is applied. For example, one day we may see micropumps made of biocompatible materials that can utilize fuels directly from the human body. These pumps may degrade into completely harmless products after their service, achieving a high level of biocompatibility.

Acknowledgements

ZC, LZ and WW are grateful for the financial support from the National Natural Science Foundation of China (grant no. 11402069) and the City Government of Shenzhen (grant no. KQCX20140521144102503).

Notes and references

1 G. M. Whitesides, *Nature*, 2006, **442**, 368–373.
2 Z. Bo, J. D. Tice, L. S. Roach and R. F. Ismagilov, *Angew. Chem.*, 2004, **116**, 2509–2509.
3 R. S. Ramsey and J. M. Ramsey, *Anal. Chem.*, 1997, **69**, 1174–1178.
4 P. S. Dittrich and M. Andreas, *Nat. Rev. Drug Discovery*, 2006, **5**, 210–218.
5 P. S. Dittrich and M. Andreas, *Anal. Bioanal. Chem.*, 2005, **382**, 1771–1782.
6 A. R. Wheeler, W. R. Throndset, R. J. Whelan, A. M. Leach, R. N. Zare, L. Yish Hann, F. Kevin, I. D. Manger and D. Antoine, *Anal. Chem.*, 2003, **75**, 3581–3586.
7 E. K. Sackmann, A. L. Fulton and D. J. Beebe, *Nature*, 2014, **507**, 181–189.
8 D. Maillefer, S. Gamper, B. Frehner, P. Balmer, H. van Lintel and P. Renaud, *The 14th IEEE International Conference on MEMS*, Interlaken, 2001.
9 V. Singhal and S. V. Garimella, *Sens. Actuators, A*, 2007, **134**, 650–659.
10 R. L. Hartman and K. F. Jensen, *Lab Chip*, 2009, **9**, 2495–2507.
11 T. A. Franke and W. Achim, *ChemPhysChem*, 2008, **9**, 2140–2156.
12 P. Abgrall and A. M. Gué, *J. Micromech. Microeng.*, 2007, **17**, R15–R49(35).
13 D. J. Beebe, G. A. Mensing and G. M. Walker, *Annu. Rev. Biomed. Eng.*, 2002, **4**, 261–286.
14 F. Amirouche, Y. Zhou and T. Johnson, *Microsyst. Technol.*, 2009, **15**, 647–666.
15 B. D. Iverson and S. V. Garimella, *Microfluid. Nanofluid.*, 2008, **5**, 145–174.
16 D. J. Laser and J. G. Santiago, *J. Micromech. Microeng.*, 2004, **14**, R35–R64.
17 S. Y. Tang, K. Khoshmanesh, V. Sivan, P. Petersen, A. P. O'Mullane, D. Abbott, A. Mitchell and K. Kalantar-zadeh, *Proc. Natl. Acad. Sci. U. S. A.*, 2014, **111**, 3304–3309.
18 C. Zhang, X. Da and Y. Li, *Biotechnol. Adv.*, 2007, **25**, 483–514.
19 H. Suzuki, A. Kumagai, K. Ogawa and E. Kokufuta, *Biomacromolecules*, 2004, **5**, 486–491.
20 T. Atsushi, K. Kenichi and S. Hiroaki, *Anal. Chem.*, 2010, **82**, 6870–6876.
21 I. M. Glynn, *J. Physiol.*, 1993, **462**, 1–30.
22 S. Sanchez, L. Soler and J. Katuri, *Angew. Chem., Int. Ed.*, 2015, **54**, 1414–1444.
23 W. Wang, W. T. Duan, S. Ahmed, T. E. Mallouk and A. Sen, *Nano Today*, 2013, **8**, 531–554.

24 D. Patra, S. Sengupta, W. T. Duan, H. Zhang, R. Pavlick and A. Sen, *Nanoscale*, 2013, **5**, 1273–1283.
25 W. T. Duan, W. Wang, S. Das, V. Yadav, T. E. Mallouk and A. Sen, *Annu. Rev. Anal. Chem*, 2015, **8**, 311–333.
26 T. R. Kline, W. F. Paxton, Y. Wang, D. Velegol, T. E. Mallouk and A. Sen, *J. Am. Chem. Soc.*, 2005, **127**, 17150–17151.
27 W. F. Paxton, K. C. Kistler, C. C. Olmeda, A. Sen, S. K. St. Angelo, Y. Cao, T. E. Mallouk, P. E. Lammert and V. H. Crespi, *J. Am. Chem. Soc.*, 2004, **126**, 13424–13431.
28 W. Wang, T. Y. Chiang, D. Velegol and T. E. Mallouk, *J. Am. Chem. Soc.*, 2013, **135**, 10557–10565.
29 Y. Wang, R. M. Hernandez, D. J. Bartlett, J. M. Bingham, T. R. Kline, A. Sen and T. E. Mallouk, *Langmuir*, 2006, **22**, 10451–10456.
30 T. C. Lee, M. Alarcón-Correa, C. Miksch, K. Hahn, J. G. Gibbs and P. Fischer, *Nano Lett.*, 2014, **14**, 2407–2412.
31 A. Nourhani, P. E. Lammert, V. H. Crespi and A. Borhan, *Phys. Fluids*, 2015, **27**, 012001.
32 Y. Solomentsev and J. L. Anderson, *J. Fluid Mech.*, 1994, **279**, 197–215.
33 J. L. Anderson, *Annu. Rev. Fluid Mech.*, 1989, **21**, 61–99.
34 S. Qian and Y. Ai, *Electrokinetic Particle Transport in Micro-/Nanofluidics: Direct Numerical Simulation Analysis*, CRC Press, Boca Raton, 2012.
35 Y. R. Luo, *Handbook of Bond Dissociation Energies in Organic Compounds*, CRC Press, Boca Raton, 2002.
36 J. A. Dean, *Lange's Handbook of Chemistry*, McGraw-Hill, New York, 1998.
37 T. R. Kline, J. Iwata, P. E. Lammert, T. E. Mallouk, A. Sen and D. Velegol, *J. Phys. Chem. B*, 2006, **110**, 24513–24521.
38 A. A. Farniya, M. J. Esplandiu, D. Reguera and A. Bachtold, *Phys. Rev. Lett.*, 2013, **111**, 168301.
39 I. K. Jun and H. Hess, *Adv. Mater.*, 2010, **22**, 4823–4825.
40 M. E. Ibele, Y. Wang, T. R. Kline, T. E. Mallouk and A. Sen, *J. Am. Chem. Soc.*, 2007, **129**, 7762–7763.
41 M. J. Esplandiu, A. A. Farniya and A. Bachtold, *ACS Nano*, 2015, **9**, 11234–11240.
42 H. Mizoguchi, M. Ando, T. Mizuno, T. Takagi and N. Nakajima, *Proceedings of IEEE MEMS*, 1992.
43 A. Terray, J. Oakey and D. W. M. Marr, *Science*, 2002, **296**, 1841–1844.
44 S. Maruo and H. Inoue, *Appl. Phys. Lett.*, 2006, **89**, 144101.
45 A. Sen, M. E. Ibele, Y. Hong and D. Velegol, *Faraday Discuss.*, 2009, **143**, 15–27.
46 R. A. Pavlick, S. Sengupta, T. McFadden, H. Zhang and A. Sen, *Angew. Chem., Int. Ed.*, 2011, **50**, 9374–9377.
47 Y. Hong, M. Diaz, U. M. Córdova-Figueroa and A. Sen, *Adv. Funct. Mater.*, 2010, **20**, 1568–1576.
48 M. E. Ibele, T. E. Mallouk and A. Sen, *Angew. Chem., Int. Ed.*, 2009, **48**, 3308–3312.
49 W. T. Duan, M. E. Ibele, R. Liu and A. Sen, *Eur. Phys. J. E: Soft Matter Biol. Phys.*, 2012, **35**, 493–501.
50 J. J. McDermott, A. Kar, M. Daher, S. Klara, G. Wang, A. Sen and D. Velegol, *Langmuir*, 2012, **28**, 15491–15497.
51 V. Yadav, H. Zhang, R. Pavlick and A. Sen, *J. Am. Chem. Soc.*, 2012, **134**, 15688–15691.
52 H. Zhang, K. Yeung, J. S. Robbins, R. A. Pavlick, M. Wu, R. Liu, A. Sen and S. T. Phillips, *Angew. Chem., Int. Ed.*, 2012, **51**, 2400–2404.
53 Y. Hua, J. Kyubong, K. L. Kounovsky, J. J. Pablo and D. C. Schwartz, *J. Am. Chem. Soc.*, 2009, **131**, 5722–5722.
54 H. S. Muddana, S. Sengupta, T. E. Mallouk, A. Sen and P. J. Butler, *J. Am. Chem. Soc.*, 2010, **132**, 2110–2111.
55 S. Sengupta, D. Patra, I. Ortiz-Rivera, A. Agrawal, S. Shklyaev, K. K. Dey, U. Cordova-Figueroa, T. E. Mallouk and A. Sen, *Nat. Chem.*, 2014, **6**, 415–422.
56 I. Ortiz-Rivera, H. Shum, A. Agrawal, A. Sen and A. C. Balazs, *Proc. Natl. Acad. Sci. U. S. A.*, 2016, **113**, 2585–2590.
57 H. Zhang, W. T. Duan, M. Q. Lu, X. Zhao, S. Shklyaev, L. Liu, T. J. Huang and A. Sen, *ACS Nano*, 2014, **8**, 8537–8542.
58 S. Sengupta, M. M. Spiering, K. K. Dey, W. T. Duan, D. Patra, P. J. Butler, R. D. Astumian, S. J. Benkovic and A. Sen, *ACS Nano*, 2014, **8**, 2410–2418.
59 D. Patra, H. Zhang, S. Sengupta and A. Sen, *ACS Nano*, 2013, **7**, 7674–7679.
60 A. A. Solovev, M. Yongfeng, B. U. A. Esteban, H. Gaoshan and O. G. Schmidt, *Small*, 2009, **5**, 1688–1692.
61 J. G. Gibbs and Y. P. Zhao, *Appl. Phys. Lett.*, 2009, **94**, 163104.
62 M. Xuan, J. Shao, X. Lin, L. Dai and Q. He, *ChemPhysChem*, 2014, **15**, 2189–2189.
63 H. Wang, G. Zhao and M. Pumera, *J. Am. Chem. Soc.*, 2014, **136**, 2719–2722.
64 Y. H. Choi, U. S. Sang and S. S. Lee, *Sens. Actuators, A*, 2004, **111**, 8–13.
65 A. A. Solovev, S. Sanchez, Y. Mei and O. G. Schmidt, *Phys. Chem. Chem. Phys.*, 2011, **13**, 10131–10135.
66 L. Soler, V. Magdanz, V. M. Fomin, S. Sanchez and O. G. Schmidt, *ACS Nano*, 2013, **7**, 9611–9620.
67 W. Duan, R. Liu and A. Sen, *J. Am. Chem. Soc.*, 2013, **135**, 1280–1283.
68 A. A. Farniya, M. J. Esplandiu and A. Bachtold, *Langmuir*, 2014, **30**, 11841–11845.